Gefitinib Induction of *In vivo* Detectable Signals by Bcl-2/Bcl-x_L Modulation of Inositol Trisphosphate Receptor Type 3

Antonella Zannetti,[1] Francesca Iommelli,[1] Rosa Fonti,[1] Angela Papaccioli,[1] Jvana Sommella,[1] Anna Lettieri,[1] Giuseppe Pirozzi,[2] Roberto Bianco,[3] Giampaolo Tortora,[3] Marco Salvatore,[1,4] and Silvana Del Vecchio[1,4]

Abstract

Purpose: To test whether epidermal growth factor receptor (EGFR) tyrosine kinase inhibitors (TKI) induce detectable signals in tumor cells and whether such signals may reveal alterations of the apoptotic program.

Experimental Design: Tumor cells were treated with gefitinib or erlotinib and tested for their ability to accumulate 99mTc-Sestamibi, a radiolabeled lipophilic cation that localizes in mitochondria. Then we tested whether Bcl-2 and Bcl-x_L alter the pattern of drug-dependent tracer accumulation while reducing tumor cell sensitivity to EGFR TKIs. The mechanism underlying the pattern of tracer accumulation was elucidated. Finally, imaging studies were done in animal models and lung cancer patients before and after treatment with EGFR TKIs using single-photon emission computed tomography and 99mTc-Sestamibi.

Results: Gefitinib increases accumulation of 99mTc-Sestamibi in Bcl-2–overexpressing cells and enhances the physical interaction of phosphorylated Bcl-2 with inositol trisphosphate receptor type 3 (IP3R3). Consequently, a relative increase of cytosolic and mitochondrial calcium levels occurs. Similarly, lung cancer cells showed an increase of tracer uptake and an enhanced interaction of Bcl-x_L with IP3R3 on exposure to erlotinib concentrations achievable in plasma. The occurrence of these interactions was associated with an enhanced EGFR TKI–induced apoptosis resistance. Posttreatment imaging studies in nude mice bearing control and Bcl-2–overexpressing breast carcinomas showed a high tumor uptake of the tracer whereas baseline studies failed to visualize tumors. Similarly, an enhancement of tracer uptake could be detected in patients with lung cancer treated with erlotinib.

Conclusion: EGFR TKIs generate detectable signals by Bcl-2/Bcl-x_L modulation of IP3R3 in tumor cells.

Aberrant expression and activation of the epidermal growth factor receptor (EGFR) is commonly found in human tumors of epithelial origin where it promotes tumor growth and progression. Therefore, many efforts have been focused on the development of specific EGFR inhibitors as innovative approaches for treatment of solid tumors. Gefitinib is a low molecular weight tyrosine kinase inhibitor (TKI) that competes for ATP binding to the catalytic kinase domain of EGFR, thus inhibiting EGF-stimulated receptor autophosphorylation and downstream signaling pathways. This ultimately results in down-regulation of many cellular processes including proliferation, survival, migration, and adhesion (1, 2). Although previous studies showed a high selectivity for EGFR-tyrosine kinase activity, a proteomic analysis identified more than 20 putative kinase targets of gefitinib, including calcium/calmodulin-dependent protein kinase II, c-jun NH_2-terminal kinase 2, breast tumor kinase, and Rip-like interacting caspase-like apoptosis-regulatory protein kinase (3).

Previous preclinical and clinical studies indicate that gefitinib response is not associated with the level of EGFR protein expression (4–6). Many factors may affect tumor response to gefitinib, which include the presence of mutated receptors (7, 8), dimerization partners (9), levels of activating ligands, and activation of downstream signaling pathways (10, 11). In particular, cells with activating mutations of EGFR exhibit dramatically high sensitivity to gefitinib and erlotinib treatment, suggesting that they are "addicted" to activated EGFR signaling (12). When treated with concentrations of gefitinib that are achievable in the plasma, these cells undergo apoptosis rather than growth arrest (5, 11). Furthermore, mutant EGFR is reported to preferentially activate the Akt and signal transducer and activator of transcription antiapoptotic signaling pathways (11). On the other hand, BH3-only proapoptotic proteins

Authors' Affiliations: [1]Institute of Biostructures and Bioimages, National Research Council; [2]Department of Experimental Oncology, National Cancer Institute; and [3]Departments of Endocrinology and Molecular and Clinical Oncology and [4]Biomorphological and Functional Sciences, University of Naples "Federico II," Naples, Italy

Received 2/12/08; revised 4/22/08; accepted 4/26/08.

Grant support: EU grant European Molecular Imaging Laboratories Network contract no 503569, Ministero della Salute, and Ministero dell'Universita' e della Ricerca.

The costs of publication of this article were defrayed in part by the payment of page charges. This article must therefore be hereby marked *advertisement* in accordance with 18 U.S.C. Section 1734 solely to indicate this fact.

Requests for reprints: Silvana Del Vecchio, Department of Biomorphological and Functional Sciences, University of Naples "Federico II," Edificio 10, Via Sergio Pansini, 5, 80131 Naples, Italy. Phone: 39-81-746-3307; Fax: 39-81-545-7081; E-mail: delvecc@unina.it.

doi:10.1158/1078-0432.CCR-08-0374

such as Bim and Bad were reported to mediate TKI-induced killing of lung cancer cells with oncogenic EGFR mutations and Bcr/Abl$^+$ leukemic cells (13, 14). Unfortunately, despite the high responsiveness of tumors bearing activating EGFR mutations, most may become resistant to TKIs due to secondary mutations occurring in the EGFR kinase domain (9, 15–17). However, it remains unknown whether secondary mutations alone may confer resistance to gefitinib or alternative mechanisms may be involved (18, 19), including those affecting key downstream mediators of the TKI-induced apoptotic program (20).

Apoptosis is often regulated by signals arising from or converging on intracellular organelles such as mitochondria and endoplasmic reticulum (ER). Both proapoptotic and antiapoptotic members of Bcl-2 family are key regulators of mitochondrial-dependent apoptosis. Their opposing actions control the mitochondrial membrane permeabilization, the release of cytochrome *c* from mitochondria, and the subsequent activation of effector caspases (21). There is growing evidence that Bcl-2 family controls apoptosis from the ER by regulating Ca^{2+} dynamics and cross talk with mitochondria (22–24). In particular, the antiapoptotic proteins Bcl-2 and Bcl-x_L, which localize to both ER and mitochondria (25), have a key role in this interorganelle cross talk. When phosphorylated, Bcl-2 predominantly localizes to the ER and is unable to bind proapoptotic Bcl-2 family proteins including Bim, Bid, and Bad (22). Conversely, Bcl-2 is reported to physically interact with all isoforms of inositol trisphosphate receptor (IP3R; refs. 23, 24), an ER-resident Ca^{2+} release channel that regulates cytoplasmic free Ca^{2+} concentration by releasing stored Ca^{2+} from ER lumen on binding of its ligand inositol 1,4,5-trisphosphate (IP3). By interacting with IP3R, Bcl-2 directly or indirectly controls the phosphorylation status and Ca^{2+} leak through this receptor (23, 24). Similarly, Bcl-x_L binds to IP3Rs to enhance Ca^{2+} release from ER stores and increases the apparent sensitivity of all IP3R isoforms to subsaturating levels of IP3 (26). Consequently, levels of Ca^{2+} in the ER lumen are likely reduced and the amount of Ca^{2+} taken up by mitochondria is not enough to allow activation of the mitochondrial permeability transition pore and cytochrome *c* release.

99mTc-Sestamibi is a radiolabeled tumor-seeking agent clinically used in a variety of human tumors including breast and lung cancer. It belongs to a class of lipophilic cations that accumulate in the mitochondria of cancer cells in response to large electronegative potentials of plasma and mitochondrial membranes (27). In previous studies, we found that high Bcl-2 levels dramatically reduced early uptake of 99mTc-Sestamibi in cultured tumor cell lines (28) and human breast carcinomas (29). Breast cancer cells stably transfected with human *Bcl-2* gene showed a 4- to 5-fold reduction of 99mTc-Sestamibi uptake as compared with control cells. Interestingly, tracer uptake was markedly enhanced in Bcl-2–overexpressing cancer cells early after treatment with staurosporine, which is an inducer of apoptosis but also a general protein kinase inhibitor. These observations prompted us to test the effect of TKIs currently approved for clinical use.

Here, we tested whether tumor cell exposure to gefitinib causes changes in 99mTc-Sestamibi uptake and whether such changes can be detected *in vivo* and eventually reveal dysregulation of the TKI-activated apoptotic program.

Materials and Methods

Cell lines and treatment. T47D, MCF-7, MDA-MB-231 human breast carcinoma, SKLU-1 human lung adenocarcinoma, A549 human non–small cell lung cancer, PC3 human prostate cancer, and A431 human epithelial carcinoma cell lines were grown in DMEM (Gibco Life Technologies) containing 10% fetal bovine serum, 100 IU/mL penicillin, and 50 μg/mL streptomycin in a humidified incubator in 5% CO_2 at 37°C. Three non–small-cell lung cancer (NSCLC) cell lines with oncogenic mutations of EGFR [i.e., H1650 with deletion of exon 19 (delE746_A750) and PTEN loss, HCC827 with deletion of exon 19 (delE746_A750), and H1975 with point mutations in exon 21 (L858R) and exon 20 (T790M)] were obtained from American Type Culture Collection. In addition, the human breast cancer cell line MCF-7 TH, selected for resistance to Adriamycin and expressing high levels of P-glycoprotein (Pgp), was grown and maintained in 200 ng/mL Adriamycin. T47D breast cancer cells were stably transfected with a plasmid containing the full-length cDNA of the human *Bcl-2* gene (T47D-Bcl-2) or with the empty vector (T47D-neo) as described elsewhere (28). Cells were treated with increasing concentration of gefitinib ranging between 0.5 and 20 μmol/L for different time intervals (range, 30 min-5 h). Parallel experiments were also done with erlotinib, an EGFR inhibitor structurally related to gefitinib. A panel of Src kinase inhibitors (PP2, genestein, and herbimycin), mitogen-activated protein kinase inhibitors (SB2035, U0126, and PD98059), and Akt kinase inhibitors (wortmannin, triciribine, and LY294002) were also tested in some cell lines. When indicated, cells were starved overnight and then incubated with 10 nmol/L EGF for 15 min. Cells were also treated with 2 μmol/L thapsigargin for 10 min either alone or in combination with gefitinib.

Drug-induced growth inhibition was assessed by using the 3-(4,5-dimethylthiazol-2yl)-5-(3-carboxymethoxy-phenyl)-2-(4-sulfophenyl)-2*H* tetrazolium (MTS) assay (Promega). This colorimetric method allows to determine the number of viable cells based on the bioreduction of MTS to formazan. This product is soluble in tissue culture medium and can be detected spectrophotometrically. Briefly, cells were seeded at a density of 5,000 to 10,000 per well in 96-well flat-bottomed plates and allowed to attach for 24 h. Cells were then treated with increasing concentrations of gefitinib or erlotinib for 72 h at 37°C. After 3-h incubation with MTS, absorbance was read at a wavelength of 490 nm. The data are expressed as percentage of viable cells, considering the untreated control cells as 100%. In addition, the extent of cell death was assessed by Annexin V-FITC-propidium iodide staining (Pharmingen).

Immunoprecipitation and immunoblot analysis. Whole-cell lysates and membrane fractions were prepared as previously described (30). Briefly, cells were lysed in 200 μL of a buffer containing 1 mmol/L EDTA, 0.2% Triton X-100, and protease and phosphatase inhibitors (lysis buffer). The suspension was homogenized by passages through a 26-gauge needle and centrifuged at 13,000 × *g* for 10 min at 4°C. Membrane fractions were obtained by resuspending cells in an isotonic buffer [20 mmol/L Tris-HCl (pH 7.6), 1 mmol/L EDTA, 1 mmol/L EGTA, protease and phosphatase inhibitors] followed by homogenization and centrifugation for 10 min at 800 × *g*. The supernatant was ultracentrifuged for 45 min at 46,000 × *g* and the resulting pellet containing the membrane fraction was collected.

Precleared proteins from cell lysates (1 mg) were incubated overnight at 4°C with 4 μg/mL of anti-IP3R3, anti–Bcl-2, or anti–Bcl-x_L monoclonal antibodies. The immunoprecipitated proteins recovered by absorption to EZview Red Protein A Affinity Gel (Sigma) were separated by SDS-PAGE, transferred to polyvinylidene difluoride membranes, and probed for the indicated proteins.

Western blot analysis of proteins from whole-cell lysates and membrane fractions was carried out using a standard procedure. Polyvinylidene difluoride membranes were probed by using the following monoclonal antibodies: anti–EGFR-P (Cell Signalling; 0.1 μg/mL),

anti-Pgp (C219 Signet; 1.5 μg/mL), anti–breast cancer resistance protein (BCRP; Chemicon; 1.5 μg/mL), anti–Bcl-2 (Santa Cruz Biotechnology; 0.2 μg/mL), anti–Bcl-x_L (Santa Cruz Biotechnology; 0.4 μg/mL), anti-IP3R3 (BD Biosciences PharMingen; 0.25 μg/mL), anti-actin (Sigma; 1 μg/mL), anti–α-tubulin (Sigma; 1 μg/mL), anti-PARP (BD Biosciences Pharmingen; 1 μg/mL), and anti-calcineurin (BD Bioscience Pharmingen; 1 μg/mL). Rabbit polyclonal antibodies against EGFR (Santa Cruz Biotechnology; 1:1,000), P-Bcl-2 (Cell Signalling; 1:1,000), Bim (Cell Signalling; 1:500), Bad (Cell Signalling; 1:1,000), and calnexin (Stressgen Biotechnologies; 1:1,000) were also used.

Intracellular Ca^{2+} and mitochondrial membrane potential measurements. Cytosolic and mitochondrial calcium levels were measured using Fluo-4-AM (5 μmol/L) and Rhod-2-AM (2.5 μmol/L) fluorescent dyes (Molecular Probes), respectively. The mitochondrial transmembrane potential ($\Delta\Psi_m$) was measured using the cationic fluorescent dye tetramethylrhodamine ethyl ester (final concentration, 50 nmol/L; Molecular Probes), which normally accumulates in mitochondria as a direct function of $\Delta\Psi_m$.

Briefly, 5×10^5 cells were washed twice in Ca^{2+}-free PBS, loaded with fluorescent dyes for 30 min at 37°C, and washed twice in Ca^{2+}-free PBS. Cells were then resuspended in phenol red–free medium supplemented with 1% fetal bovine serum and subjected to treatment with 20 μmol/L gefitinib, 2 μmol/L thapsigargin, or 50 μmol/L carbonylcyanide *m*-chlorophenylhydrazone (CCCP) for the indicated time period. Finally, cells were washed and resuspended in Ca^{2+}-free PBS, and the fluorescence intensities were measured using a Becton-Dickinson FACScan flow cytometer.

RNA interference. IP3R3, Bcl-2, and Pgp targeting siRNA pools, along with the corresponding control nontargeting siRNA pools, were purchased from Dharmacon. Control and Bcl-2–overexpressing T47D cells were transfected using DharmaFECT siRNA transfection reagent and 100 nmol/L siRNAs according to the manufacturer's protocol. Cells were grown in culture after transfection for 48 to 72 h before use in experiments, and down-regulation of targeted protein expression was assessed by Western blot analysis.

99mTc-Sestamibi uptake in cultured tumor cells. Cells were plated at a density of 100,000 to 200,000 per well in 12-well flat-bottomed plates in 500 μL of medium and allowed to grow for 2 d. Sestamibi (Cardiolite, Bristol-Myers Squibb) was labeled with 99mTc according to the manufacturer's instructions.

When subconfluent, cells were incubated with 37 kBq of 99mTc-Sestamibi in 500 μL of medium for 60 min at 37°C in triplicates. Nonspecific binding was determined in wells containing only medium and never exceeded 0.2% of total radioactivity. Cells were rinsed twice in ice-cold PBS and then lysed with 1 mol/L NaOH to recover cell-associated radioactivity, which was determined using a standard gamma counter. The percentage of radioactivity specifically associated to the cells was expressed as the ratio between the specific cell uptake (after subtraction of nonspecific binding) and the total radioactivity added in each well. Protein concentration was determined in each sample and tracer uptake was normalized for protein content. All the assays were done in triplicates.

Animal tumor model and micro-single photon emission computed tomography imaging. Male BALB/c (nu/nu) mice, 5 weeks old and weighing 15 to 20 g, were purchased from Charles River Laboratories. All animal experiments were approved by the local Animal Care and Use Committee. T47D human breast cancer cells stably transfected with cDNA of human *Bcl-2* gene and mock-transfected cells (1×10^7) were resuspended in 200-μL DMEM and injected s.c. into opposite flanks of individual mice. This experimental approach was adopted to test whether tracer uptake, assessed in basal conditions in each tumor, changes after gefitinib treatment in the same animal. The use of untreated individual tumor as its own control after therapy contributes to limit the experimental variability. Cells were then allowed to grow for 2 wk, and tumors with a diameter ranging between 0.3 and 1 cm were obtained. Each tumor-bearing mouse underwent a baseline micro-single photon emission computed tomography (SPECT) study, then was treated with 150 mg/kg/d gefitinib orally for 3 d and underwent a second microSPECT study after treatment. Briefly, mice were anesthetized and 99mTc-Sestamibi was i.v. injected through the tail vein. After 1 h, microSPECT images were obtained using the YAP-(S)PET scanner (ISE). The data were acquired in list mode from 256 views over an angle of 360 degrees. Images were then reconstructed using an iterative reconstruction algorithm that provided transaxial, coronal, and sagittal slices. At the end of the second microSPECT study, animals were sacrificed and tumors were removed for radioactivity counting. A subgroup of animals was subjected to biodistribution studies before and after gefitinib treatment. The animals were sacrificed 1 h postinjection; blood and major organs including heart, liver, spleen, lung, and kidneys were collected, wet-weighed, and counted in a gamma counter. Organ and tumor uptake was expressed as the percentage of injected dose per gram of tissue.

Imaging in lung cancer patients. Three patients (two male and one female, age 50-69 y) with NSCLC refractory to chemotherapy and candidate for treatment with EGFR TKIs were studied. All human studies were done on approval by the local Ethical Committee and all patients gave their informed consent. They were i.v. injected with 740 MBq of 99mTc-Sestamibi and subjected to whole body scan and SPECT imaging of the chest using a double-headed gamma camera (ECAM, Siemens) equipped with low-energy high-resolution collimators. SPECT images were acquired in a 128 × 128 matrix using 60 projections, 25 s/projection, and then reconstructed using an iterative algorithm. After the baseline study, patients were treated for 3 d with 150-mg erlotinib orally and underwent a posttreatment imaging study following the same protocol described above.

Statistics. Data were summarized as mean ± SD, and the statistical significance of differences between means was assessed by using unpaired Student's *t* test. Differences between means were considered statistically significant at $P < 0.05$.

Results

Gefitinib-dependent accumulation of radiolabeled cationic compounds in a panel of cultured tumor cell lines and Bcl-2–overexpressing cells. We preliminarily tested the effects of gefitinib on 99mTc-Sestamibi uptake in a panel of cultured tumor cell lines showing a large spectrum of EGFR and P-EGFR levels (Fig. 1A). Tracer uptake was assessed in basal conditions and after cell exposure to 20 μmol/L gefitinib or 1 μmol/L cetuximab for 1 hour (Fig. 1B). Although absolute uptake of the tracer was different among tumor cell lines, treatment with gefitinib, but not cetuximab, caused a 2- to 2.5-fold increase of 99mTc-Sestamibi uptake in all the cell lines tested, except MCF-7, which showed a 50% increase. These findings indicate that gefitinib enhances accumulation of radiolabeled lipophilic cations in cultured tumor cell lines and that this enhancement is independent of EGFR expression and EGF-induced receptor activation. Conversely, cetuximab, which has a different mechanism of EGFR inhibition, is not able to alter tracer uptake.

Then the effect of gefitinib was tested in control (T47D-neo) and Bcl-2–overexpressing T47D cells (T47D-Bcl-2). This breast cancer cell line had been stably transfected with the human *Bcl-2* gene (28) and, as expected, showed the highest levels of Bcl-2 expression as compared with all the cell lines tested (Fig. 2A, *left*). Furthermore, high levels of Bcl-2 protected transfected cells from gefitinib-induced apoptosis [Fig. 2A (*middle*) and B]. Because Pgp is known to interfere with 99mTc-Sestamibi uptake in cultured tumor cell lines (31) and gefitinib was reported to interact with both Pgp and BCRP (32–34), cells were also screened for Pgp and BCRP by Western

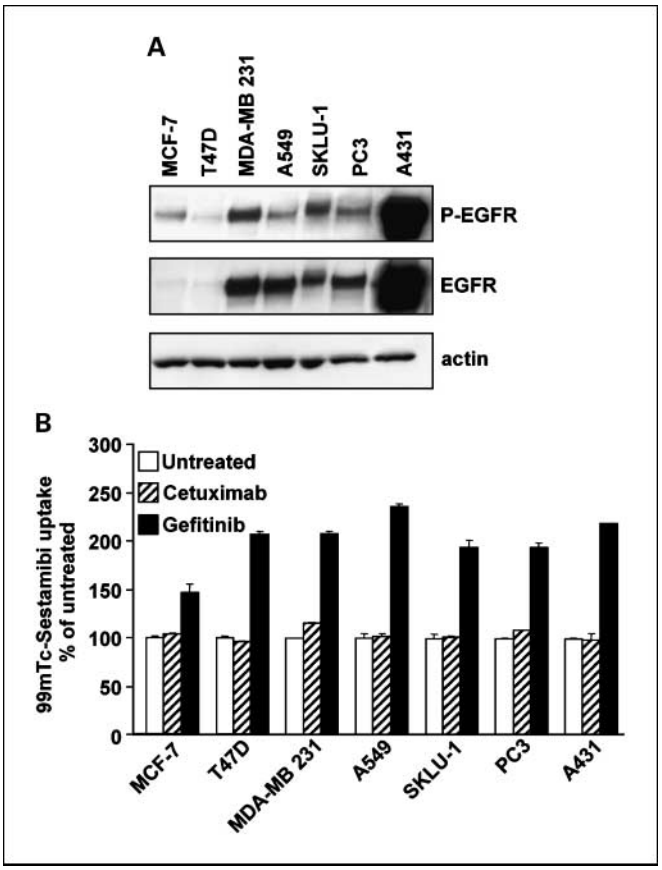

Fig. 1. Gefitinib-dependent accumulation of radiolabeled cationic compounds in a panel of cultured tumor cell lines. *A,* levels of EGFR and P-EGFR were determined in whole-cell lysates of different cultured tumor cells. Equal amounts of proteins (90 μg) were separated by 3% to 8% SDS-PAGE and immunoblotted for P-EGFR, EGFR, and actin. To induce EGFR autophosphorylation, cells had been starved overnight and then incubated with 10 nmol/L EGF. *B,* uptake of 99mTc-Sestamibi, a lipophilic cation with mitochondrial localization, was assessed in tumor cell lines in basal conditions and after treatment with 1 μmol/L cetuximab or 20 μmol/L gefitinib for 1 h. No enhancement of tracer uptake was observed on cell exposure to cetuximab. Conversely, gefitinib caused a 2- to 2.5-fold increase of 99mTc-Sestamibi uptake in all the cell lines tested except MCF-7.

blot analysis. No detectable levels of Pgp or BCRP were found in T47D-neo and T47D-Bcl-2 (Fig. 2A, *right*).

Control and Bcl-2–overexpressing T47D cells were incubated with increasing concentration of gefitinib ranging between 0.5 and 20 μmol/L, the latter being a concentration much higher than levels achievable in patients (Fig. 2C, *left*). Similarly to the other tumor cell lines tested, a 2-fold increase of tracer uptake was observed in control cells. In agreement with our previous findings, Bcl-2–overexpressing cells accumulate less 99mTc-Sestamibi than control cells in basal conditions. However, treatment with increasing concentration of gefitinib caused up to a 4-fold increase of tracer uptake that nevertheless remained lower than in treated control cells. Time course experiments showed that the effect of gefitinib on both control and Bcl-2–overexpressing cells occurred as early as 30 minutes (Fig. 2C, *right*).

Then we tested whether other kinase inhibitors can cause the same effect on 99mTc-Sestamibi uptake in control and Bcl-2–overexpressing cells. Mitogen-activated protein kinase inhibitors (SB203580, UO126, and PD98059) and Src kinase inhibitors (PP2, genistein, and herbimycin) did not cause any significant change in tracer uptake in both control and Bcl-2–overexpressing cells, whereas among the Akt kinase inhibitors (wortmannin, triciribine, and LY294002), LY294002 caused a 60% increase of tracer uptake in both cell lines (data not shown). None of these kinase inhibitors affected cell viability as assessed by MTS assay.

Effect of gefitinib on ER-mitochondria cross talk. Because Bcl-2 is reported to interact with IP3R, thus regulating redistribution of Ca^{2+} from ER to mitochondria, we tested whether gefitinib causes an enhancement of Bcl-2 binding to IP3R and whether such interaction may affect intracellular Ca^{2+} dynamics and, consequently, mitochondrial accumulation of radiolabeled cationic compounds. Immunoprecipitation with anti-IP3R3 antibody of whole-cell lysates from untreated and gefitinib-treated cells followed by Western blot analysis with an antibody against phosphorylated Bcl-2 showed that gefitinib treatment causes an increase of phosphorylated Bcl-2 that physically interacts with IP3R3 (Fig. 3A, *left*) Immunoprecipitation with anti–Bcl-2 antibody followed by Western blot with anti-IP3R3 antibody confirmed the enhancement of Bcl-2 and IP3R3 interaction on exposure to gefitinib (Fig. 3A, *right*). The interaction of phosphorylated Bcl-2 with IP3R1 was not tested due to the low level of this isoform in T47D cells.

In agreement with these findings, both control and Bcl-2–overexpressing cells showed a relative increase of cytosolic and mitochondrial Ca^{2+} levels after 1-hour treatment with gefitinib, indicating the induction of an IP3R3-mediated calcium release with a secondary relative increase of mitochondrial calcium uptake (Fig. 3B, *left* and *middle*). Thapsigargin, an irreversible inhibitor of the sarcoplasmic reticulum Ca^{2+} ATPase (SERCA) responsible for uptake of Ca^{2+} from the cytosol into the ER lumen, was used as positive control. In both control and Bcl-2–overexpressing cells, a mild hyperpolarization of mitochondrial membrane occurred in response to 1-hour treatment with gefitinib, whereas the uncoupler CCCP, used as positive control, induced a prompt depolarization (Fig. 3B, *right*). Conversely, cell exposure to gefitinib for 24 hours caused depolarization of mitochondrial membrane in control cells, whereas Bcl-2–overexpressing cells showed preserved mitochondrial membrane potentials (data not shown). Taken together, these findings indicate that Ca^{2+} signals arising from ER of control and Bcl-2–overexpressing cells in response to gefitinib are similar in nature, although they may differ in amplitude and efficacy to promote activation of mitochondrial permeability transition pore.

Ca^{2+} release from ER usually activates calcineurin, a Ca^{2+}/calmodulin-dependent phosphatase that in turn may dephosphorylate Bad (35) and activate downstream caspases. However, when Bcl-2 is overexpressed, active calcineurin is reported to be sequestered from its natural substrates, likely including also IP3R, by binding to Bcl-2 (36). Therefore, we tested whether gefitinib treatment may also influence the interaction of Bcl-2 with calcineurin. Immunoprecipitation with anti–Bcl-2 antibody of whole-cell lysates of untreated and treated T47D-Bcl-2 cells followed by blotting with anti-calcineurin antibody showed that Bcl-2 and calcineurin interaction is enhanced by gefitinib treatment, indicating a relocation of calcineurin in Bcl-2 domain on drug exposure (Fig. 3C, *left*). To test whether endogenously expressed Bcl-2 may interact with calcineurin on exposure to gefitinib, we examined the lung cancer cell line SKLU-1 containing detectable endogenous levels

of Bcl-2. Immunoprecipitation of whole-cell lysates of untreated and treated cells showed an enhanced binding of calcineurin to Bcl-2 in gefitinib-treated SKLU-1 cells (Fig. 3C, *right*).

Gefitinib-dependent tracer uptake and intracellular Ca^{2+} dynamics. To prove that gefitinib-dependent modulation of IP3R3 function is responsible for the observed enhanced uptake of 99mTc-Sestamibi, IP3R3 expression was down-regulated by transfecting control and Bcl-2–overexpressing T47D cells with IP3R3 targeting siRNA. Scrambled nontargeting siRNA was used as negative control. Suppression of IP3R3 expression (Fig. 4A) significantly reduced gefitinib-dependent enhancement of tracer uptake in both cell lines (Fig. 4B). Interestingly, down-regulation of IP3R3 completely abolished the enhancement of tracer uptake in response to 1 μmol/L gefitinib, a concentration achievable in the plasma.

To test whether the interaction of Bcl-2 with IP3R3 is required for gefitinib-dependent changes in tracer uptake, its expression was suppressed by transfecting T47D-Bcl-2 cells with targeting siRNA. Although limited, a significant reduction of tracer uptake was observed on down-regulation of Bcl-2 expression, indicating that the interaction of this antiapoptotic protein with IP3R3 contributes to the ER-mitochondrial redistribution of the tracer in response to gefitinib (Fig. 4A and C). Despite the absence of detectable levels of Pgp in T47D-Bcl-2 cells, we wanted to exclude that even undetectable levels of Pgp may affect our results. Therefore, T47D-Bcl-2 cells were transfected with Pgp targeting siRNA pools that efficiently lowered protein levels in Pgp-overexpressing MCF-7 TH cells (Fig. 4A). No significant changes in tracer uptake could be observed after transfection of Pgp targeting siRNA in response to gefitinib (Fig. 4C).

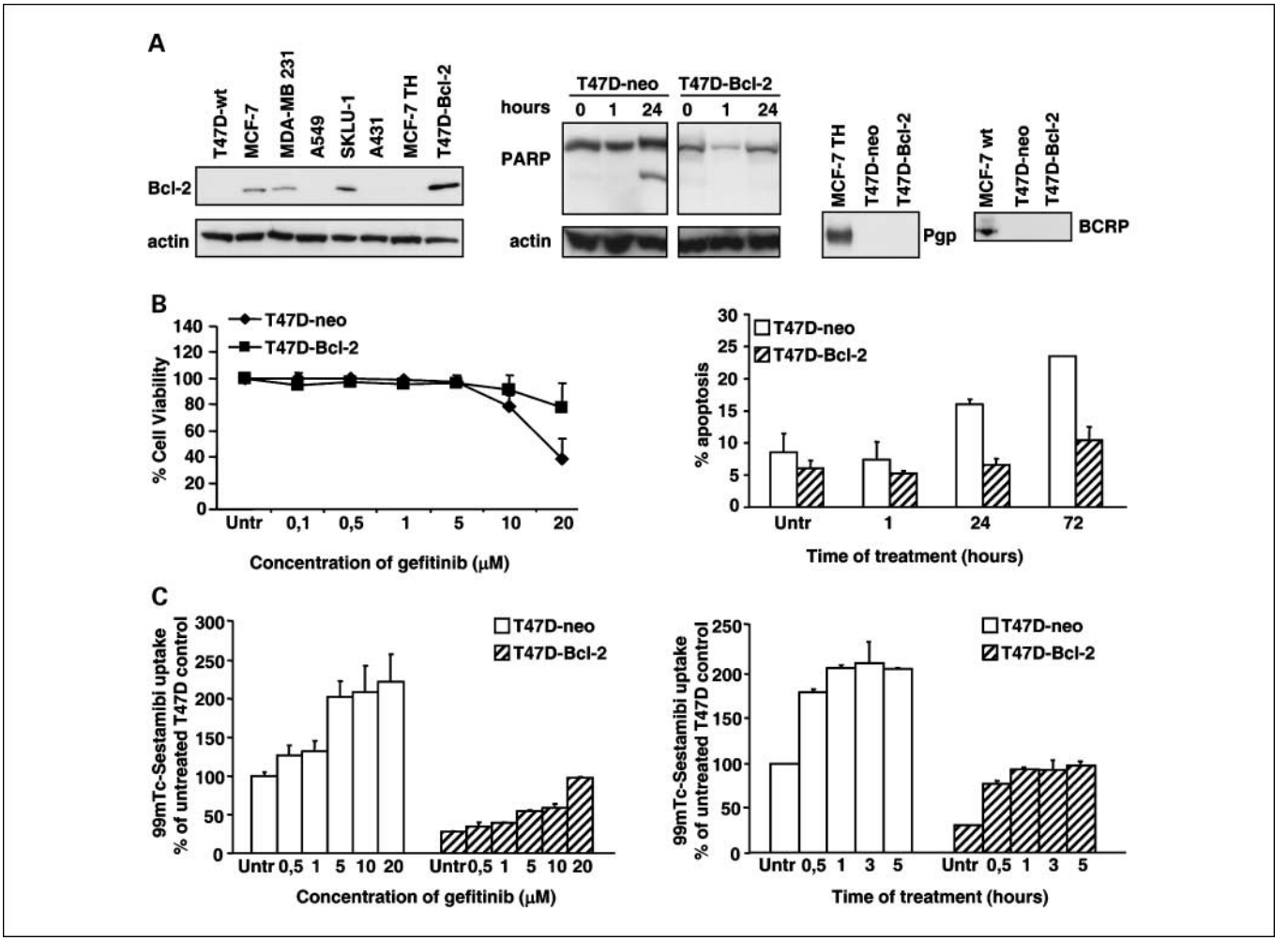

Fig. 2. Altered pattern of gefitinib-dependent tracer uptake in Bcl-2–overexpressing cells. T47D breast cancer cells had been stably transfected with a plasmid containing the full-length cDNA of the human *Bcl-2* gene (T47D-Bcl-2) or with the empty vector (T47D-neo). *A,* left, protein samples (30 μg) from whole-cell lysates were separated by 10% SDS-PAGE and immunoblotted for Bcl-2 and actin. Among all the tumor cell lines tested, T47D-Bcl-2 showed the highest levels of Bcl-2. Middle, PARP cleavage was assessed in control and Bcl-2–overexpressing T47D cells exposed to 20 μmol/L gefitinib up to 24 h. Right, membrane fractions (70 μg) were separated by 7% or 10% SDS-PAGE and immunoblotted for Pgp and BCRP. *B,* left, MTS assay was done in control and Bcl-2–overexpressing T47D cells to assess cell viability after 72-h treatment with increasing concentrations of gefitinib. Right, percentage of apoptotic breast cancer cells positively stained with Annexin V-FITC was determined during 72-h treatment with 20 μmol/L gefitinib. *C,* left, T47D-neo and T47D-Bcl-2 breast cancer cells were incubated with increasing concentration of gefitinib ranging between 0.5 and 20 μmol/L. 99mTc-Sestamibi uptake was determined and expressed as percentage of untreated T47D-neo cells. In basal conditions, Bcl-2–overexpressing breast cancer cells showed a lower uptake of radiolabeled cationic compounds as compared with control cells. When exposed to increasing concentrations of gefitinib, T47D-Bcl-2 cells showed up to a 4-fold increase of tracer uptake, whereas a 2-fold increase was observed in control cells. Right, 99mTc-Sestamibi uptake was determined in breast cancer cells treated with 20 μmol/L gefitinib for different time intervals. The gefitinib-enhanced uptake of radiolabeled cationic compounds in both control and Bcl-2–overexpressing cells was detected as early as 30 min.

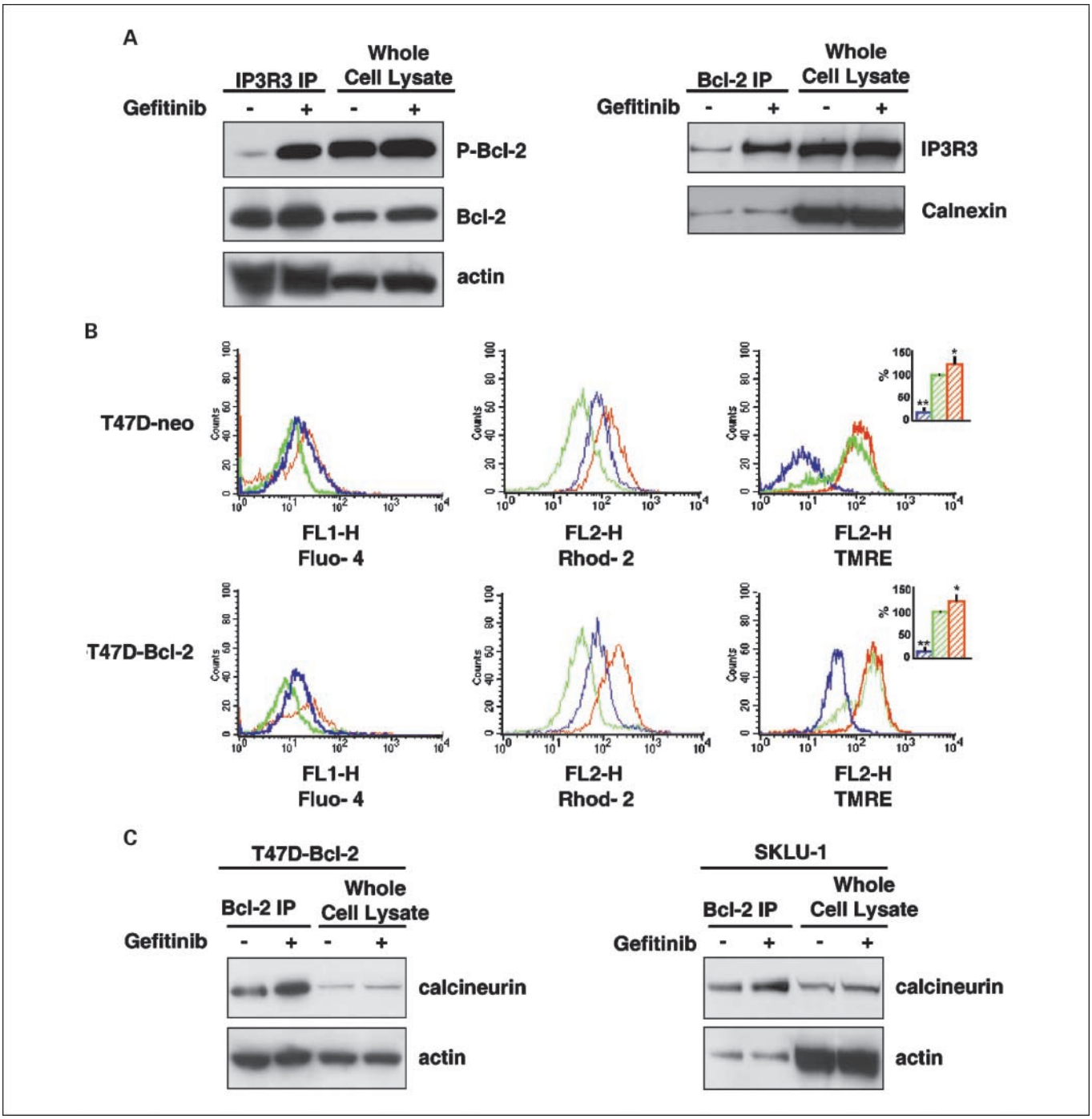

Fig. 3. Enhancement of the physical interaction of P-Bcl-2 with IP3R3 and relative increase of cytosolic and mitochondrial Ca^{2+} levels in response to gefitinib. *A,* left, T47D-Bcl-2 breast cancer cells were treated with 20 μmol/L gefitinib for 1 h. Whole-cell lysates obtained from untreated and treated T47D-Bcl-2 cells were immunoprecipitated with anti-IP3R3 and immunoblotted for P-Bcl-2 and Bcl-2. Gefitinib treatment enhanced the physical interaction between phosphorylated Bcl-2 and IP3R3. Right, immunoprecipitation with anti – Bcl-2 antibody followed by immunoblotting with anti-IP3R3 antibody confirmed the enhancement of the interaction between Bcl-2 and IP3R3 on exposure to gefitinib. *B,* control and Bcl-2 – overexpressing T47D cells were treated with 20 μmol/L gefitinib for 1 h, 2 μmol/L thapsigargin for 10 min, or 50 μmol/L CCCP for 3 min. Cytosolic (*left*) and mitochondrial (*middle*) Ca^{2+} levels were assessed using Fluo-4-AM and Rhod-2-AM, respectively. Cells were analyzed by flow cytometry. Untreated, gefitinib-treated, and thapsigargin-treated cells are shown in green, red, and blue, respectively. The enhancement of fluorescence intensity on FL-1 and FL-2 channel indicates a relative increase of cytosolic and mitochondrial Ca^{2+} levels, respectively, in treated cells as compared with untreated control cells. The mitochondrial transmembrane potential ($\Delta\Psi_m$; *right*) was measured after 1-h gefitinib treatment by flow cytometry using the cationic fluorescent dye tetramethylrhodamine ethyl ester, which accumulates in mitochondria as a direct function of $\Delta\Psi_m$. Untreated, gefitinib-treated, and CCCP-treated cells are shown in green, red, and blue, respectively. Top and bottom graphs, results of a representative experiment in T47D-neo and T47D-Bcl-2 cells respectively. Gefitinib treatment caused a 36% and 25% increase of fluorescence intensity in control and Bcl-2 – overexpressing cells, respectively, indicating a mild hyperpolarization. Conversely, the positive control CCCP induced depolarization, showing a 88% and 77% decrease of fluorescent intensity in control and Bcl-2 – overexpressing cells, respectively. Inset, data from four independent experiments were pooled and expressed as percentage of untreated corresponding cells (*columns,* mean; *bars,* SD). *, $P < 0.05$; **, $P < 0.001$, unpaired Student's *t* test. *C,* whole-cell lysates of untreated and gefitinib-treated T47D-Bcl-2 and SKLU-1 cells were immunoprecipitated with anti – Bcl-2 antibody and then subjected to Western blot analysis with anti-calcineurin antibody. Gefitinib treatment enhances the interaction between Bcl-2 and calcineurin, indicating the relocation of calcineurin in the same membrane compartment of Bcl-2. Actin and calnexin were used to ensure equal loading.

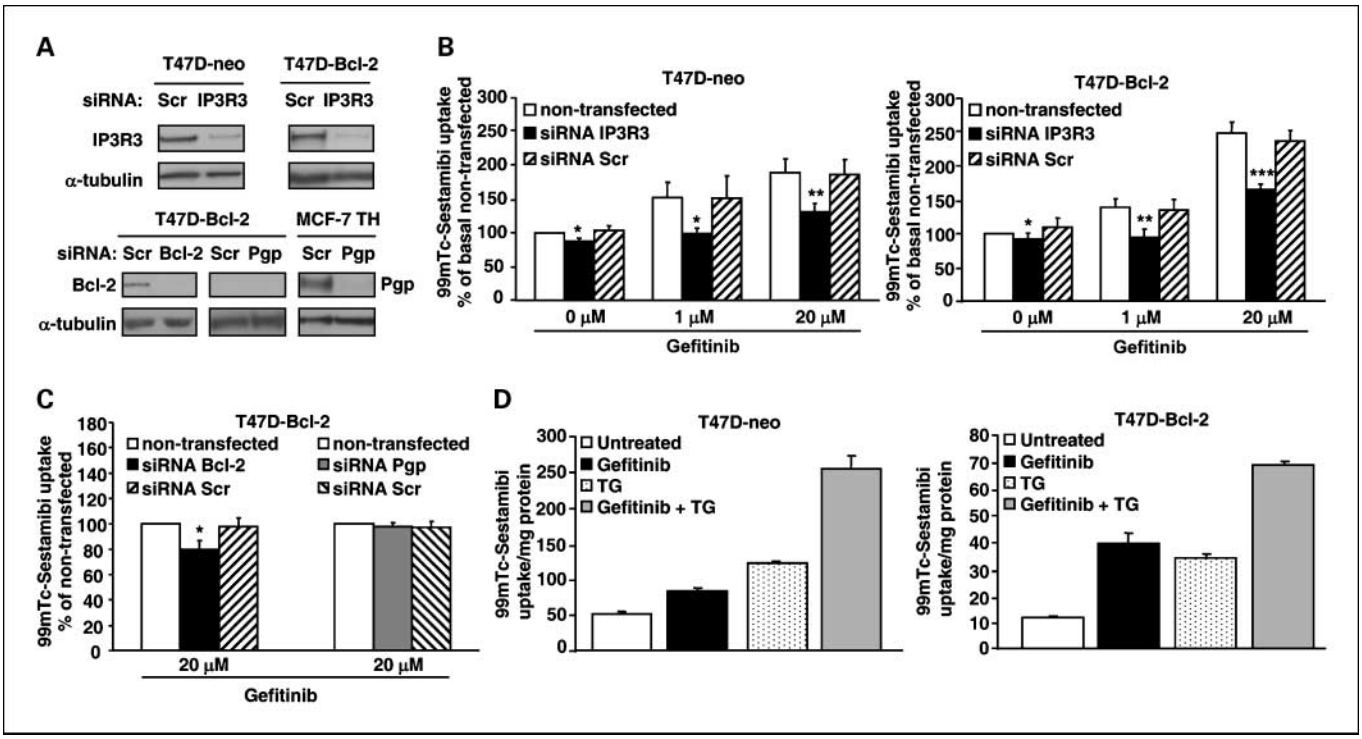

Fig. 4. Gefitinib-dependent uptake of radiolabeled cationic compounds and intracellular Ca^{2+} dynamics. *A,* the expression of IP3R3, Bcl-2, and Pgp was efficiently suppressed by transfecting the indicated cell lines with protein targeting siRNA pools using corresponding scrambled siRNA pools as negative control (*Scr*). Protein levels were analyzed by Western blotting. *B,* 99mTc-Sestamibi uptake (expressed as percentage of basal nontransfected corresponding cell line) was then assessed in nontransfected, IP3R3 targeting siRNA – transfected, and scrambled siRNA – transfected T47D-neo (*left*) and T47D-Bcl-2 (*right*) cells. Suppression of IP3R3 expression significantly reduced gefitinib-dependent enhancement of tracer uptake as compared with scrambled siRNA – transfected cells, indicating that the expression of this Ca^{2+} release channel is required for the enhanced accumulation of the tracer on exposure to gefitinib in both cell lines. *C,* T47D-Bcl-2 cells were transfected with Bcl-2 or Pgp targeting siRNA using the corresponding scrambled siRNA as negative control and then exposed to 20 μmol/L gefitinib. 99mTc-Sestamibi uptake (expressed as percentage of nontransfected, gefitinib-treated T47D-Bcl-2 cells) was then assessed in nontransfected, targeting siRNA – transfected, and scrambled siRNA – transfected cells. A significant reduction of 99mTc-Sestamibi uptake was observed on suppression of Bcl-2 expression, whereas Pgp targeting siRNA transfection did not cause any significant change in tracer uptake. *D,* 99mTc-Sestamibi uptake (expressed as percentage of cell-associated radioactivity per milligram of protein) was determined after treatment with 20 μmol/L gefitinib (1 h), 2 μmol/L thapsigargin (10 min), and 20 μmol/L gefitinib (1 h) plus 2 μmol/L thapsigargin (10 min) in control (*left*) and Bcl-2 – overexpressing (*right*) T47D cells. Thapsigargin caused an increase of tracer uptake similar to that obtained with gefitinib in both control and Bcl-2 – overexpressing cells, although in a different scale of uptake values. The combined treatment showed an additive effect between gefitinib and thapsigargin. Columns, mean from three independent experiments; bars, SD. *, $P < 0.05$; **, $P < 0.005$; ***, $P < 0.0001$, unpaired Student's *t* test.

To further confirm that gefitinib-induced changes in 99mTc-Sestamibi uptake reflect intracellular Ca^{2+} dynamics, we tested tracer uptake in response to acute inhibition of Ca^{2+} uptake into the ER lumen by thapsigargin that ultimately results in an almost complete depletion of ER Ca^{2+} stores. Thapsigargin caused an increase of tracer uptake similar to that obtained with gefitinib in both control and Bcl-2 – overexpressing T47D cells (Fig. 4D). Notably, the scale of tracer uptake variation was considerably lower in Bcl-2 – overexpressing cells than in control cells, in agreement with a reduced thapsigargin-releasable Ca^{2+} pool previously reported in Bcl-2 – overexpressing cells (37, 38), and associated with a reduced susceptibility to apoptosis. Furthermore, the combined treatment with gefitinib and thapsigargin caused a strong enhancement of tracer uptake that was higher than that determined by the treatment with gefitinib or thapsigargin alone in both control and Bcl-2 – overexpressing cells, indicating that there is an additive effect between the two drugs and that the targets of gefitinib and thapsigargin do not work in a linear pathway to control tracer uptake.

Imaging of gefitinib-modulated Ca^{2+} dynamics in tumor xenografts. Nude mice bearing control and Bcl-2 – overexpressing breast carcinomas on the right and left flank, respectively, were subjected to microSPECT with 99mTc-labeled lipophilic cations before and after treatment with gefitinib. All baseline studies failed to detect control and Bcl-2 – overexpressing tumors. In agreement with *in vitro* findings, both tumors could be visualized after treatment with gefitinib in all animals, although tracer uptake, expressed as percentage of injected dose per gram of tumor, was 2-fold higher in control as compared with Bcl-2 – overexpressing tumors. Representative images of the microSPECT studies are shown in Fig. 5. Coronal sections of the inferior region of the body of the same animal before (*left*) and after (*right*) treatment with gefitinib were analyzed with normal (*top*) and enhanced (*bottom*) contrast. No tumor uptake could be observed in the baseline study even with the use of contrast-enhanced images. Conversely, T47D-neo tumor was detected after treatment using normal contrast. Despite the minute size, the Bcl-2 – overexpressing tumor could be visualized in contrast-enhanced images. The biodistribution and plasma clearance of the tracer assessed in a subgroup of animals were not altered by treatment with gefitinib (data not shown).

Detection of EGFR TKI – induced signals in NSCLC cells and in lung cancer patients. Because the plasma concentration achievable in mice treated with gefitinib may be much higher than that achievable in patients with lung cancer, we wanted to

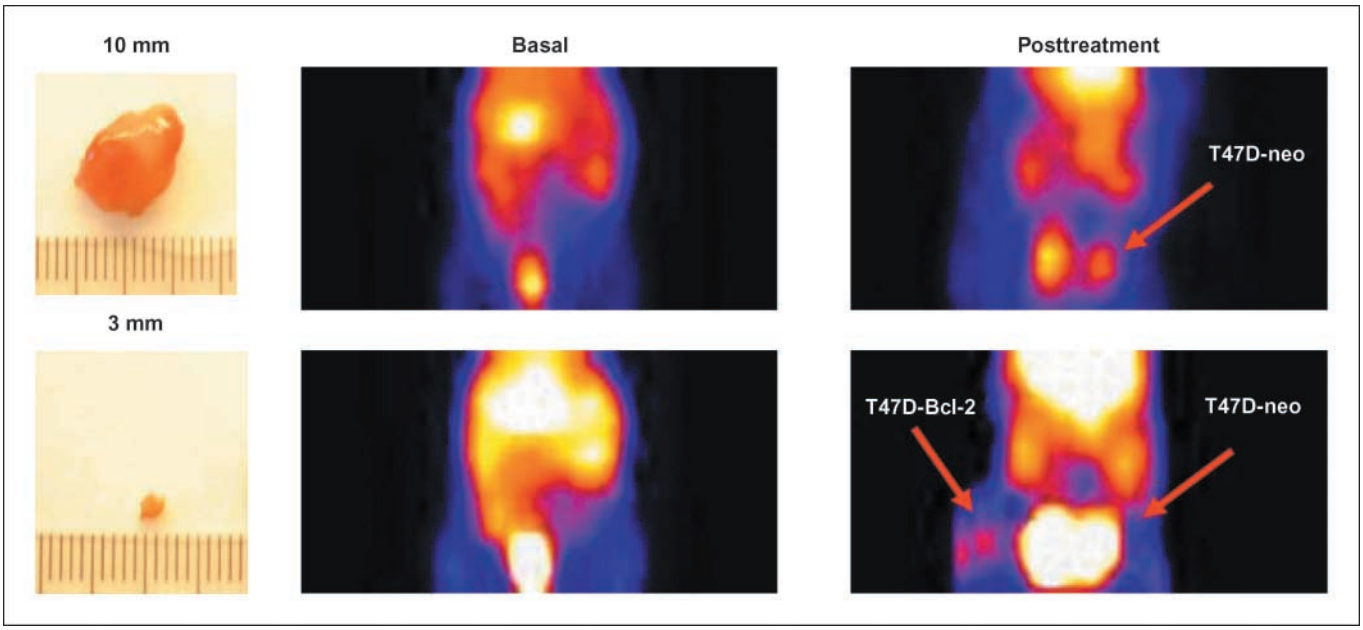

Fig. 5. Detection of gefitinib-modulated Ca^{2+} dynamics in tumor xenografts. Nude mice bearing control and Bcl-2–overexpressing T47D cells on the right and left flank, respectively, were subjected to microSPECT with 99mTc-Sestamibi before and after oral administration of 150 mg/kg/d gefitinib for 3 d. Representative images of the microSPECT studies. Coronal sections of the inferior region of the body of the same animal before (*left*) and after (*right*) treatment with gefitinib were analyzed with normal (*top*) and enhanced (*bottom*) contrast. No tumor uptake could be observed in the baseline study even with the use of contrast-enhanced images. Conversely, T47D-neo tumor was detected after treatment using normal contrast whereas the Bcl-2–overexpressing tumor could be visualized in contrast-enhanced images. Left, sizes of T47D-neo (*top*) and T47D-Bcl-2 (*bottom*) tumors.

test whether treatment with TKI induces detectable signals also in lung cancer patients, thus eventually revealing dysregulation of TKI-induced apoptotic program. Because lung cancer patients who are candidate for TKI treatment received erlotinib at our institution, the patients enrolled for the imaging studies were treated with erlotinib instead of gefitinib. Therefore, we preliminarily tested the effect of increasing concentration of erlotinib on tracer uptake in NSCLC cells with EGFR mutations showing a large spectrum of sensitivity to erlotinib (Fig. 6A). In fact, despite the presence of activating mutations in all cell lines (delE746_A750 or L858R), H1975 cells harbor also a T790M mutation, known to confer resistance to gefitinib and erlotinib (15, 17), whereas H1650 are reported to be resistant due to an impaired up-regulation of Bim in response to EGFR TKI (13, 20, 39). The NSCLC H1650 cells showed a 2.7-fold enhancement of tracer uptake at erlotinib concentration of 0.5 μmol/L whereas higher concentrations of the drug were required to induce a similar enhancement of tracer uptake in HCC827 and H1975 cells (Fig. 6B). The prompt enhancement of tracer uptake at TKI concentration achievable in the plasma was associated with resistance to erlotinib treatment in H1650 cells that showed indeed a high cell viability (Fig. 6A) and absence of PARP cleavage in response to erlotinib treatment (Fig. 6C, *top*). Furthermore, no detectable levels of Bcl-2 were found in HCC827, H1975, and H1650 cells whereas Bcl-x_L showed a variable but detectable expression in the same lung cancer cell lines (Fig. 6C, *middle*). Consequently, we tested whether Bcl-x_L was able to interact with IP3R3 on exposure to TKI and found an enhancement of such interaction in response to 1 μmol/L erlotinib in H1650, which was confirmed at 20 μmol/L erlotinib (Fig. 6C, *bottom*). In agreement with these observations and as previously reported (13, 20, 39), H1650 cells did not show detectable levels of the BH3-only proapoptotic protein Bim, a condition that may lead to the unopposed action of Bcl-x_L in this cell line, whereas the presence of Bim_{EL} isoform in HCC827 and H1975 cells may counteract Bcl-x_L (Fig. 6C, *middle*).

Imaging studies in lung cancer patients showed a strong enhancement of 99mTc-Sestamibi in one of three patients after treatment with erlotinib for 3 days. A 4-cm tumor in the apical region of the left lung was not visible in the baseline study and showed a peripheral enhancement of tracer uptake in the posttreatment scan corresponding to viable tumor tissue, as shown by the fluorodeoxyglucose positron emission tomography done in the same patient before treatment with erlotinib (Fig. 6D). This patient showed disease progression 5 months later and erlotinib treatment was discontinued.

Discussion

In this study, we found that gefitinib generates ER-modulated signals in cancer cells, which are independent of EGFR expression but rather involve members of Bcl-2 family regulating apoptosis and IP3 receptors modulating Ca^{2+} homeostasis. In the presence of high levels of Bcl-2, gefitinib, used at concentrations higher than those usually achievable in plasma, enhances the physical interaction of phosphorylated Bcl-2 with IP3R3 in the ER and increases the IP3R3-mediated calcium release with a secondary increase of mitochondrial calcium uptake. In addition, calcineurin is relocated in Bcl-2 membrane compartment after treatment with gefitinib. Similarly, NSCLC cells with oncogenic EGFR mutations and undetectable levels of Bcl-2 show an enhanced interaction between Bcl-x_L and IP3R3 on erlotinib exposure. This ultimately results in an enhanced TKI-induced apoptosis resistance in both cell types.

In agreement with these observations, previous studies reported that Bcl-2 and IP3R1 physically interact at the ER and their binding is increased in the absence of Bax and Bak (23), a condition mimicking the presence of unbalanced high levels of Bcl-2. Despite their functional differences, all isoforms of IP3R were found to interact with Bcl-2 (24) and Bcl-x_L (26, 40). To the best of our knowledge, this is the first report on the interaction between Bcl-2/Bcl-x_L and IP3Rs occurring in the ER on exposure to EGFR TKIs.

In addition to Bcl-2/Bcl-x_L, other members of Bcl-2 family as well as other downstream mediators of TKI-induced apoptosis may have a role in the occurrence of the events described. In this respect, BH3-only proapoptotic member Bim has been reported to mediate TKI-induced apoptosis in sensitive EGFR-mutant cells (13) and Bcr/Abl$^+$ leukemic cells (14). Knockdown of Bim by siRNA reduced gefitinib-induced apoptosis; more importantly, gefitinib-dependent up-regulation of Bim is blocked by secondary mutations in the catalytic kinase domain of EGFR (13). In this context, the unopposed action of high levels of Bcl-2/Bcl-x_L may generate IP3R-mediated signals that can be suitable for imaging purposes. In addition, other isoforms of IP3R may be involved in the interaction with Bcl-2/Bcl-x_L. The expression of individual IP3R isoforms varies among cell types and may give rise to functional redundancy

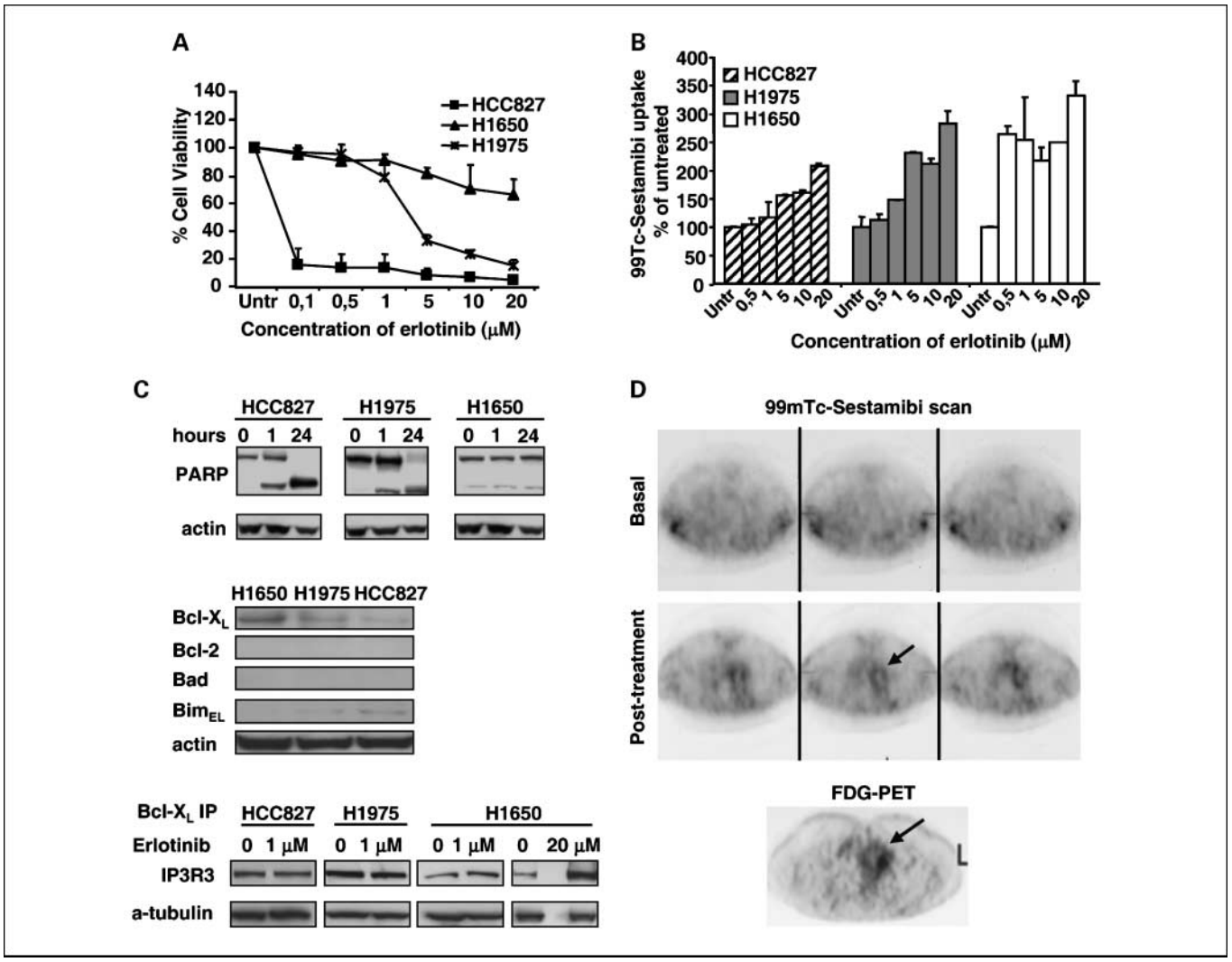

Fig. 6. EGFR TKI – induced Bcl-x_L interaction with IP3R3 in NSCLC cells and imaging in lung cancer patients. The NSCLC cell lines HCC827, H1975, and H1650 bearing oncogenic mutations of EGFR (see Materials and Methods) were selected and tested for sensitivity to erlotinib and uptake of 99mTc-Sestamibi. *A,* MTS assay done in lung cancer cells after 72-h treatment with increasing concentrations of erlotinib showed a lower sensitivity of H1650 cells to treatment as compared with HCC827 and H1975. *B,* 99mTc-Sestamibi uptake was determined in HCC827, H1975, and H1650 NSCLC cells in the presence of increasing concentration of erlotinib ranging between 0.5 and 20 μmol/L. H1650 cells showed a 2.7-fold enhancement of tracer uptake at erlotinib concentration of 0.5 μmol/L, whereas higher concentrations of erlotinib were required to induce a similar enhancement of tracer uptake in HCC827 and H1975 cells. *C,* top, PARP cleavage was assessed in NSCLC cells exposed to 20 μmol/L erlotinib up to 24 h. No PARP cleavage in response to erlotinib could be observed in H1650, confirming that, despite the presence of oncogenic EGFR mutations, this cell line was resistant to erlotinib treatment. Middle, NSCLC cell lines were tested for Bcl-x_L, Bcl-2, Bad, and Bim expression by Western blotting analysis. Bim_{EL}, Bim extra long isoform. Bottom, NSCLC cells bearing oncogenic EGFR mutations were treated with 1 μmol/L erlotinib for 1 h. Whole-cell lysates obtained from untreated and treated lung cancer cells were immunoprecipitated with anti – Bcl-x_L antibody and immunoblotted for IP3R3 and α-tubulin. In H1650 cells, erlotinib treatment enhanced the physical interaction between Bcl-x_L and IP3R3 at 1 μmol/L, a concentration achievable in the plasma of lung cancer patients, which was confirmed at 20 μmol/L. *D,* SPECT studies were done in lung cancer patients before and after treatment with erlotinib for 3 d, and transaxial sections from a lung cancer patient are shown. A 4-cm tumor in the apical region of the left lung was not visible in the baseline study and showed a peripheral enhancement of tracer uptake in the posttreatment scan corresponding to viable tumor tissue, as shown by the fluorodeoxyglucose positron emission tomography done in the same patient before treatment with erlotinib.

or differences in their ability to modulate intracellular Ca^{2+} dynamics in response to TKI treatment.

The signals arising from ER in response to gefitinib can be detected both *in vitro* and *in vivo* by 99mTc-Sestamibi, a lipophilic cationic compound driven by plasma and mitochondrial membrane potentials. In addition to the *Nerstian* nature of this probe, our study highlighted the ability of this compound to trace intracellular calcium dynamics. Silencing IP3R expression by targeting siRNA abolished the effect of gefitinib on tracer uptake whereas thapsigargin-induced Ca^{2+} release strongly enhanced tracer uptake in both control and Bcl-2 – overexpressing cells, although in a different scale of values. The enhanced uptake of radiolabeled cationic compounds in Bcl-2 – overexpressing cells on exposure to gefitinib is associated with an increase of phosphorylated Bcl-2 interacting with IP3R3 in the ER. Suppression of Bcl-2 expression by siRNA indicates that the interaction of Bcl-2 with IP3R3 significantly contributes to gefitinib-dependent enhancement of tracer uptake. Notably, the unopposed action of high levels of Bcl-x_L in NSCLC with mutated EGFR receptor causes a similar enhancement of tracer uptake by interacting with IP3R in response to concentration of TKI achievable in the plasma, and such interaction was associated with TKI-induced apoptosis resistance. In agreement with our findings, Bcl-x_L is able to interact with all isoforms of IP3R and increases the apparent sensitivity of the receptor to subsaturating concentration of the agonist, thus causing an enhanced spontaneous Ca^{2+} signaling and apoptosis protection (26). In addition, Bcl-x_L is reported to reduce the total releasable ER Ca^{2+} pool in cells expressing type 3 IP3R and not type 2 and type 1 isoforms (26).

A potential clinical application of these findings could be the development of a responsiveness test to EGFR TKI treatment using noninvasive imaging. For instance, patients with NSCLC may undergo a SPECT study before and shortly after the beginning of EGFR TKI treatment. Because the reported drug plasma concentration achievable in patients is 1 μmol/L, a strong enhancement of tracer uptake occurring in response to the usual dose schedule would indicate resistance to EGFR TKI due to Bcl-x_L overexpression or its unopposed action. Furthermore, although our study was focused on early events occurring at the ER-mitochondria interface, another potential clinical application could be to monitor patients under EGFR TKI treatment by serial imaging. An enhancement of tracer uptake that persists in tumors over time during treatment would be indicative of EGFR TKI resistance due to Bcl-2/Bcl-x_L overexpression or their unbalanced levels. Conversely, an initial enhancement of tumor uptake that declines and disappears during treatment would be indicative of an effective apoptotic response leading to disruption of mitochondrial membrane potentials and collapse of the driving force required for tracer uptake. However, further clinical studies are needed to confirm these hypotheses and to determine the optimal time window for scanning after treatment.

Finally, our findings support the concept of "oncogene addiction" of cancer cells (12, 41). Besides the acute inhibition of EGFR signaling by gefitinib and erlotinib, an ER-mediated response is elicited in tumor cells and this would result in apoptosis if cells are highly dependent on EGFR survival signals and do not have a defective apoptotic program. Bcl-2 and Bcl-x_L play a key role in this ER-mediated response and should be taken into account when considering the cellular context in which EGFR TKIs are used. Their up-regulation or unopposed action may disrupt the efficient cross talk between ER and mitochondria, thus causing TKI-induced apoptosis resistance. Our study shows the possibility to detect *in vivo* the signals arising from gefitinib-dependent interaction between Bcl-2/Bcl-x_L and the IP3R3 Ca^{2+} release channel, thus identifying dysregulation of TKI-induced apoptosis.

Disclosure of Potential Conflicts of Interest

No potential conflicts of interest were disclosed.

Acknowledgments

We thank D. Piwnica-Worms for helpful discussions.

References

1. Ono M, Kuwano M. Molecular mechanisms of epidermal growth factor receptor (EGFR) activation and response to gefitinib and other EGFR-targeting drugs. Clin Cancer Res 2006;12:7242–51.
2. Herbst RS, Fukuoka M, Baselga J. Gefitinib—a novel targeted approach to treating cancer. Nat Rev Cancer 2004;4:956–65.
3. Brehmer D, Greff Z, Godl K, et al. Cellular targets of gefitinib. Cancer Res 2005;65:379–82.
4. Sun S, Schiller JH, Spinola M, Minna JD. New molecularly targeted therapies for lung cancer. J Clin Invest 2007;117:2740–50.
5. Johnson BE, Janne PA. Epidermal growth factor receptor mutations in patients with non-small cell lung cancer. Cancer Res 2005;65:7525–9.
6. Bianco R, Melisi D, Ciardiello F, Tortora G. Key cancer cell signal transduction pathways as therapeutic targets. Eur J Cancer 2006;42:290–4.
7. Lynch TJ, Bell DW, Sordella R, et al. Activating mutations in the epidermal growth factor receptor underlying responsiveness of non-small-cell lung cancer to gefitinib. N Engl J Med 2004;350:2129–39.
8. Paez JG, Janne PA, Lee JC, et al. EGFR mutations in lung cancer: correlation with clinical response to gefitinib therapy. Science 2004;304:1497–500.
9. Engelman JA, Janne PA, Mermel C, et al. ErbB-3 mediates phosphoinositide 3-kinase activity in gefitinib-sensitive non-small cell lung cancer cell lines. Proc Natl Acad Sci U S A 2005;102:3788–93.
10. Eberhard DA, Johnson BE, Amler LC, et al. Mutations in the epidermal growth factor receptor and in KRAS are predictive and prognostic indicators in patients with non-small-cell lung cancer treated with chemotherapy alone and in combination with erlotinib. J Clin Oncol 2005;23:5900–9.
11. Sordella R, Bell DW, Haber DA, Settleman J. Gefitinib-sensitizing EGFR mutations in lung cancer activate anti-apoptotic pathways. Science 2004;305:1163–7.
12. Weinstein IB. Cancer. Addiction to oncogenes—the Achilles heal of cancer. Science 2002;297:63–4.
13. Costa DB, Halmos B, Kumar A, et al. BIM mediates EGFR tyrosine kinase inhibitor-induced apoptosis in lung cancers with oncogenic EGFR mutations. PLoS Med 2007;4:1669–79.
14. Kuroda J, Puthalakath H, Cragg MS, et al. Bim and Bad mediate imatinib-induced killing of Bcr/Abl+ leukemic cells, and resistance due to their loss is overcome by a BH3 mimetic. Proc Natl Acad Sci U S A 2006;103:14907–12.
15. Pao W, Miller VA, Politi KA, et al. Acquired resistance of lung adenocarcinomas to gefitinib or erlotinib is associated with a second mutation in the EGFR kinase domain. PLoS Med 2005;2:e73.
16. Kwak EL, Sordella R, Bell DW, et al. Irreversible inhibitors of the EGF receptor may circumvent acquired resistance to gefitinib. Proc Natl Acad Sci U S A 2005;102:7665–70.
17. Kobayashi S, Boggon TJ, Dayaram T, et al. EGFR mutation and resistance of non-small-cell lung cancer to gefitinib. N Engl J Med 2005;352:786–92.
18. Engelman JA, Zejnullahu K, Mitsudomi T, et al. MET amplification leads to gefitinib resistance in lung cancer by activating ERBB3 signaling. Science 2007;316:1039–43.
19. Bean J, Brennan C, Shih JY, et al. MET amplification occurs with or without T790M mutations in EGFR mutant lung tumors with acquired resistance to gefitinib or erlotinib. Proc Natl Acad Sci U S A 2007;104:20932–7.
20. Deng J, Shimamura T, Perera S, et al. Proapoptotic BH3-only BCL-2 family protein BIM connects death signaling from epidermal growth factor receptor inhibition to the mitochondrion. Cancer Res 2007;67:11867–75.

21. Reed JC. Proapoptotic multidomain Bcl-2/Bax-family proteins: mechanisms, physiological roles, and therapeutic opportunities. Cell Death Differ 2006;13:1378–86.

22. Bassik MC, Scorrano L, Oakes SA, Pozzan T, Korsmeyer SJ. Phosphorylation of BCL-2 regulates ER Ca^{2+} homeostasis and apoptosis. EMBO J 2004;23:1207–16.

23. Oakes SA, Scorrano L, Opferman JT, et al. Proapoptotic BAX and BAK regulate the type 1 inositol trisphosphate receptor and calcium leak from the endoplasmic reticulum. Proc Natl Acad Sci U S A 2005;102:105–10.

24. Chen R, Valencia I, Zhong F, et al. Bcl-2 functionally interacts with inositol 1,4,5-trisphosphate receptors to regulate calcium release from the ER in response to inositol 1,4,5-trisphosphate. J Cell Biol 2004;166:193–203.

25. Danial NN, Korsmeyer SJ. Cell death: critical control points. Cell 2004;116:205–19.

26. Li C, Wang X, Vais H, Thompson CB, Foskett JK, White C. Apoptosis regulation by Bcl-x(L) modulation of mammalian inositol 1,4,5-trisphosphate receptor channel isoform gating. Proc Natl Acad Sci U S A 2007;104:12565–70.

27. Piwnica-Worms D, Kronauge JF, Chiu ML. Uptake and retention of hexakis (2-methoxyisobutyl isonitrile) technetium(I) in cultured chick myocardial cells. Mitochondrial and plasma membrane potential dependence. Circulation 1990;82:1826–38.

28. Aloj L, Zannetti A, Caraco C, Del Vecchio S, Salvatore M. Bcl-2 overexpression prevents 99mTc-MIBI uptake in breast cancer cell lines. Eur J Nucl Med Mol Imaging 2004;31:521–7.

29. Del Vecchio S, Zannetti A, Aloj L, Caraco C, Ciarmiello A, Salvatore M. Inhibition of early 99mTc-MIBI uptake by Bcl-2 anti-apoptotic protein overexpression in untreated breast carcinoma. Eur J Nucl Med Mol Imaging 2003;30:879–87.

30. Zannetti A, Del Vecchio S, Carriero MV, et al. Coordinate up-regulation of Sp1 DNA-binding activity and urokinase receptor expression in breast carcinoma. Cancer Res 2000;60:1546–51.

31. Piwnica-Worms D, Chiu ML, Budding M, Kronauge JF, Kramer RA, Croop JM. Functional imaging of multidrug-resistant P-glycoprotein with an organotechnetium complex. Cancer Res 1993;53:977–84.

32. Yang CH, Huang CJ, Yang CS, et al. Gefitinib reverses chemotherapy resistance in gefitinib-insensitive multidrug resistant cancer cells expressing ATP-binding cassette family protein. Cancer Res 2005;65:6943–9.

33. Elkind NB, Szentpetery Z, Apati A, et al. Multidrug transporter ABCG2 prevents tumor cell death induced by the epidermal growth factor receptor inhibitor Iressa (ZD1839, Gefitinib). Cancer Res 2005;65:1770–7.

34. Nakamura Y, Oka M, Soda H, et al. Gefitinib ("Iressa", ZD1839), an epidermal growth factor receptor tyrosine kinase inhibitor, reverses breast cancer resistance protein/ABCG2-mediated drug resistance. Cancer Res 2005;65:1541–6.

35. Wang HG, Pathan N, Ethell IM, et al. Ca^{2+}-induced apoptosis through calcineurin dephosphorylation of BAD. Science 1999;284:339–43.

36. Shibasaki F, Kondo E, Akagi T, McKeon F. Suppression of signalling through transcription factor NF-AT by interactions between calcineurin and Bcl-2. Nature 1997;386:728–31.

37. Scorrano L, Oakes SA, Opferman JT, et al. BAX and BAK regulation of endoplasmic reticulum Ca^{2+}: a control point for apoptosis. Science 2003;300:135–9.

38. Palmer AE, Jin C, Reed JC, Tsien RY. Bcl-2-mediated alterations in endoplasmic reticulum Ca^{2+} analyzed with an improved genetically encoded fluorescent sensor. Proc Natl Acad Sci U S A 2004;101:17404–9.

39. Gong Y, Somwar R, Politi K, et al. Induction of BIM is essential for apoptosis triggered by EGFR kinase inhibitors in mutant EGFR-dependent lung adenocarcinomas. PLoS Med 2007;4:e294.

40. White C, Li C, Yang J, et al. The endoplasmic reticulum gateway to apoptosis by Bcl-X(L) modulation of the InsP3R. Nat Cell Biol 2005;7:1021–8.

41. Sharma SV, Bell DW, Settleman J, Haber DA. Epidermal growth factor receptor mutations in lung cancer. Nat Rev Cancer 2007;7:169–81.

Clinical Cancer Research

Gefitinib Induction of *In vivo* Detectable Signals by Bcl-2/Bcl-x_L Modulation of Inositol Trisphosphate Receptor Type 3

Antonella Zannetti, Francesca Iommelli, Rosa Fonti, et al.

Clin Cancer Res 2008;14:5209-5219.